

A New Control Strategy for Voltage-Type PWM Rectifiers to Realize Zero Steady-State Control Error in Input Current

Yukihiko Sato, *Member, IEEE*, Tomotsugu Ishizuka, Kazuyoshi Nezu, and Teruo Kataoka, *Fellow, IEEE*

Abstract— In this paper, a new simple control strategy for ac input current of voltage-type pulsewidth modulation (PWM) rectifiers which can eliminate the steady-state control error completely is proposed. This control method requires neither the instantaneous value of the supply voltage nor any accurate circuit parameters on the ac side of the rectifier. Thus, a robust operation against the variation of the circuit parameters can be achieved. In the proposed control system, a digital resonant element implemented by a digital signal processor (DSP) is introduced as a feedback controller. The digital resonant element exhibits a function similar to an integrator for the fundamental frequency components. Thus, it can eliminate the steady-state control error of the input current completely. The principle of the proposed control method is discussed, and its effectiveness is shown theoretically. The detailed method of the implementation of the lossless digital resonant element is explained. The effects of the harmonics in the supply voltage on the ac input current waveform are clarified. To confirm the effectiveness of the proposed control method, some experimental results from two laboratory test systems are shown.

Index Terms— Harmonic reduction, input current control, voltage-type pulsewidth modulation rectifier.

I. INTRODUCTION

IN RECENT YEARS, voltage-type pulsewidth modulation (PWM) rectifiers, which can realize unity input power factor and almost sinusoidal ac input current, have been widely investigated [1]–[6], and some of them have already been put into practice. In the voltage-type PWM rectifiers, the ac input current is indirectly controlled by adjusting the ac-side voltage of the bridge circuit. To achieve this, the detected instantaneous values of the supply voltage and the accurate values of the ac-side circuit parameters are required, resulting in a complicated control system configuration. If a hysteresis controller based on the instantaneous comparison of the ac input current and its reference is applied, the ac input current

Paper IPCSD 98–01, presented at the 1997 Industry Applications Society Annual Meeting, New Orleans, LA, October 5–9, and approved for publication in the IEEE TRANSACTIONS ON INDUSTRY APPLICATIONS by the Industrial Power Converter Committee of the IEEE Industry Applications Society. Manuscript released for publication February 6, 1998.

Y. Sato is with the Tokyo Institute of Technology, Tokyo, 152-8552 Japan.

T. Ishizuka was with the Tokyo Institute of Technology, Tokyo, 152-8552 Japan. He is now with the Power Electronics Development Group, Power Electronics Equipment Department, Toshiba Corporation Fuchu Works, Tokyo, 183-0043 Japan.

K. Nezu was with the Tokyo Institute of Technology, Tokyo, 152-8552 Japan. He is now with the Railway Technical Research Institute, Tokyo, 185-8540 Japan.

T. Kataoka is with Tokyo Denki University, Tokyo, 101-8457 Japan.

Publisher Item Identifier S 0093-9994(98)03619-6.

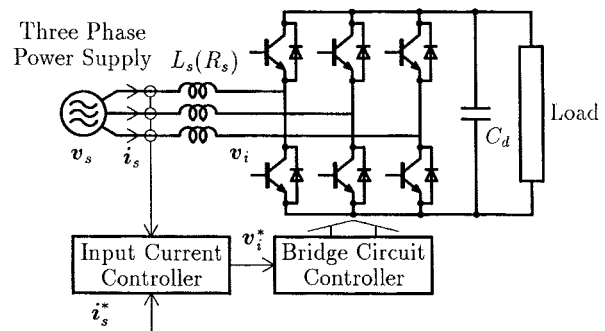


Fig. 1. Typical main circuit and control block diagram of voltage-type PWM rectifiers.

can be controlled accurately without knowledge of the supply voltage and the ac-side circuit parameters. However, the switching frequency of the power devices changes significantly during a fundamental period, resulting in the higher stress on the power devices. In addition, the total harmonic distortion becomes higher for a given value of the average switching frequency. From this point of view, the hysteresis controller is not suitable, especially for high-power applications.

In this paper, a new control strategy of the ac input current is proposed which can eliminate the steady-state control error completely without using the detected values of the supply voltage and ac-side circuit parameters. In addition, this control method can be applicable to carrier-based PWM rectifiers, in which the switching frequency is kept constant. Thus, this method is suitable also for high-power PWM rectifiers. In the proposed control circuit, a lossless digital resonant element is used as the input current controller. The control error between the input current and its reference is applied to the digital resonant element. Since it has an infinite gain at the resonant frequency, the digital resonant element exhibits a function similar to an integrator for the alternating current component, the frequency of which is equal to the resonant frequency. In this case, the resonant frequency is set to the fundamental frequency of the supply voltage. The output signal of the digital resonant element is applied to the PWM pattern generator as the reference signal for the ac-side voltage of the bridge circuit. The lossless resonant element used in the proposed control method cannot be realized by analog circuits, because power loss is not avoidable in the practical circuit components. Thus, the lossless resonant element is implemented using a digital signal processor (DSP).

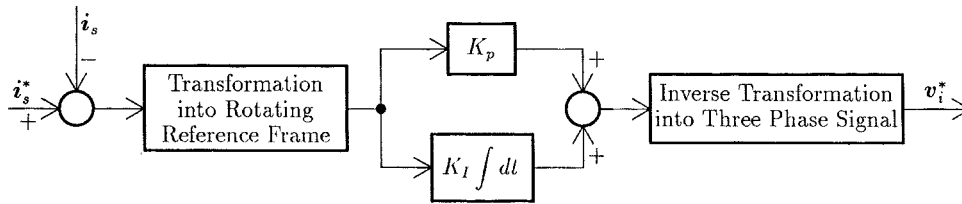


Fig. 2. Input current controller using PI controller.

So far, some control methods of voltage-type PWM rectifiers employing a proportional integral (PI) controller which can eliminate the steady-state control error of the ac input current completely have been proposed [6]. However, coordinate transformations of three-phase signals to dc signals are required, because the PI controller can eliminate the control error completely only for the dc components. This results in a complicated control system configuration. In contrast to this, the proposed control strategy can realize a simpler control algorithm without these transformations. In addition, the proposed method is suitable also for single-phase PWM rectifiers to which such coordinate transformation is not applicable.

In this paper, the control of the ac input current of the voltage-type PWM rectifiers is summarized first. Based on these investigations, the principle of the proposed control method is discussed, and its effectiveness is shown theoretically. The detailed method of the implementation of the lossless digital resonant element using a DSP is explained. The effects of the harmonics in the supply voltage on the ac input current waveform is investigated. A modification of the control system to eliminate these effects of the supply voltage harmonics is shown. To confirm the effectiveness of the proposed control method, some experimental results from two laboratory test systems are shown.

II. CONSIDERATION OF AC INPUT CURRENT CONTROL

A. Principle of AC Input Current Control in Voltage-Type PWM Rectifiers

Fig. 1 shows a typical main circuit and generalized control block diagram of the voltage-type PWM rectifiers. The ac-side voltage \mathbf{v}_i ($= [v_{iu}, v_{iv}, v_{iw}]^T$) is controlled directly by the PWM operation of the bridge circuit. The control of ac input current \mathbf{i}_s ($= [i_{su}, i_{sv}, i_{sw}]^T$) is achieved indirectly by adjusting the amplitude and phase angle of \mathbf{v}_i . In general, the current controller can be classified into feedback and feedforward controllers. The feedforward controllers are very sensitive to the variation of ac-side circuit parameters such as inductances L_s and resistances R_s of the ac inductor and ac lines. Thus, the feedforward controller cannot be a practical solution to the complete elimination of the control error in the fundamental component of the input current.

B. Conventional AC Input Current Controller

Therefore, a feedback controller should be used to eliminate the control error completely. A PI controller is one of the widely used feedback controllers. Fig. 2 shows a typical

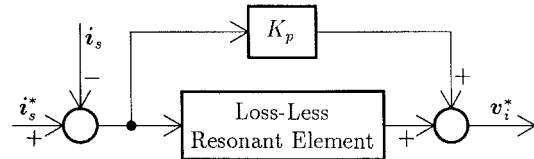


Fig. 3. Proposed input current controller using a resonant element.

control circuit configuration using the PI controller [6]. The detected signal of the input current \mathbf{i}_s and its reference signal \mathbf{i}_s^* are three phase quantities. In the case of the PI controller, the complete elimination of the steady-state control error is achieved only for the dc component. Thus, the error signal ($\mathbf{i}_s^* - \mathbf{i}_s$) must be transformed to dc signals before being applied to the PI controller. This is achieved by a coordinate transformation to the rotating reference frame which is synchronized with the frequency of the supply voltage. The output signal of the PI controller is inversely transformed to a three-phase value to generate the reference signal \mathbf{v}_i^* . These requirements of the transformation result in a complicated control algorithm. In addition, the controller shown in Fig. 2 is not applicable to single-phase PWM rectifiers, because a single-phase signal cannot be transformed to a dc signal in the manner shown in Fig. 2.

III. PROPOSED CONTROL PRINCIPLE

A. Configuration of Proposed Controller

Fig. 3 shows a new input current controller introducing a lossless resonant element proposed in this paper. The transfer function $G_r(s)$ of the lossless resonant element is given by

$$G_r(s) = \frac{K_r}{1 + (s/\omega_1)^2} \quad (1)$$

where K_r is the dc gain and ω_1 is the resonant angular frequency of the resonant element. Note that the value of $G_r(s)$ goes to infinity when $s = j\omega_1$. In this case, the resonant angular frequency ω_1 is set to the angular frequency ω_s of the supply voltage. Each phase component of the difference ($\mathbf{i}_s^* - \mathbf{i}_s$) between the supply current and its reference is applied to the resonant element as an input signal without any transformation. The output signal of the resonant element is used as a component of the reference signal of ac-side voltage \mathbf{v}_i^* . Since the transformation of the signals is not required in the proposed method, we can have a simpler control algorithm. By the function of the feedback controller shown in Fig. 3, the output signal of the resonant element is adjusted automatically to a value which makes the fundamental

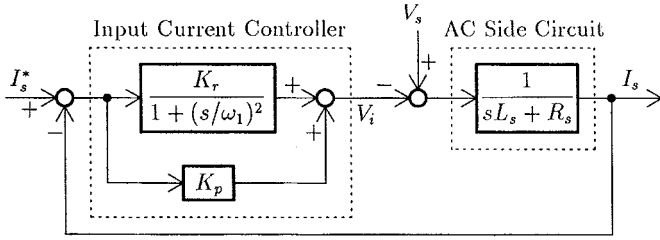


Fig. 4. Control block diagram of ac input current control system.

frequency component of the ac input current coincide exactly with its reference. When the fundamental components of the input current \hat{i}_s and its reference \hat{i}_s^* coincide exactly, the fundamental component of the input signal ($\hat{i}_s^* - \hat{i}_s$) of the resonant element becomes zero. The resonant element can sustain the generation of the reference signal v_i^* required for the input current control, even under this condition. From the above discussion, we can see that the resonant element in Fig. 3 can eliminate the steady-state error in the fundamental component of the supply current completely. From another point of view, the resonant element can be regarded as an integrator for alternating current components, frequency of which is equal to the resonant frequency. To improve transient response, a proportional controller denoted by a control gain K_p is connected in parallel with the resonant element, as shown in Fig. 3. The effectiveness of this proportional controller has been clarified in our previous paper [7]. Note that the information of the accurate circuit parameters is not required in the proposed controller. Thus, it provides the robustness against the variation in the ac-side circuit parameters.

As mentioned before, the transformation of the three phase signals into dc signals is not required in the proposed control method. Thus, it can be applied also to single-phase rectifiers.

B. Theoretical Verification of Complete Error Elimination

Fig. 4 shows the control block diagram of the proposed current control system. In Fig. 4, L_s and R_s are the inductance and resistance of the ac-side inductor, including those of the ac line. From Fig. 4, the transfer function from the reference signal I_s^* of the ac input current to its actual value I_s is given by

$$F_{ii}(s) = \frac{I_s(s)}{I_s^*(s)} = \frac{-H(s)/(sL_s + R_s)}{1 - H(s)/(sL_s + R_s)} \quad (2)$$

where $H(s)$ is the total transfer function of the proposed ac input current controller given by

$$H(s) = \frac{K_r}{1 + (s/\omega_1)^2} + K_p. \quad (3)$$

Substituting $s = j\omega_1$ into (2), we can obtain the control characteristics at the resonant frequency ω_1 :

$$\begin{aligned} F_{ii}(j\omega_1) &= \frac{I_s(j\omega_1)}{I_s^*(j\omega_1)} \\ &= \frac{\omega_1^2 K_r}{\omega_1^2 K_r} = 1. \end{aligned} \quad (4)$$

In the proposed controller, ω_1 is set to the fundamental angular frequency of the supply voltage. To obtain sinusoidal input current, the input current reference I_s^* contains only the fundamental frequency component. Thus, from (4), we can see that the fundamental frequency component in the actual input current I_s coincides exactly with its reference I_s^* in the steady state. This means that the steady-state control error in the fundamental component can be eliminated completely. In addition, we should note that $F_{ii}(j\omega_1)$ is unity, regardless of the values of the control parameters K_r, K_p , and the ac-side circuit parameters L_s, R_s . In other words, the complete elimination of the control error in the ac input current can be realized regardless of these parameters.

Similarly, from Fig. 4, we can also obtain the transfer function from the supply voltage V_s to the actual ac input current I_s as follows:

$$F_{vi}(s) = \frac{I_s(s)}{V_s(s)} = \frac{1/(sL_s + R_s)}{1 - H(s)/(sL_s + R_s)}. \quad (5)$$

Substituting $s = j\omega_1$,

$$F_{vi}(j\omega_1) = \frac{I_s(j\omega_1)}{V_s(j\omega_1)} = \frac{0}{\omega_1^2 K_r} = 0. \quad (6)$$

From this result, we can see that $F_{vi}(j\omega_1)$ is always zero, regardless of the control parameters K_r, K_p , and circuit parameters L_s, R_s . This means that the supply voltage does not affect the control characteristics of the ac input current, regardless of these parameters.

From these investigations, the effectiveness and robustness of the proposed control method have been confirmed theoretically.

IV. IMPLEMENTATION OF CONTROL SYSTEM

A. Implementation of Resonant Element

The lossless resonant element introduced in Fig. 3 cannot be realized by conventional analog circuits, because power loss is not avoidable in the practical circuit components. Thus, the lossless resonant element is implemented mathematically by a DSP. Fig. 5 shows an equivalent circuit of the resonant element. The transfer function y/u of this circuit is equal to (1) under the condition $K_r = 1$ and $\omega_1 = 1/\sqrt{L_r C_r}$. The state equation and output equation of this circuit are given by

$$\begin{aligned} \frac{dx}{dt} &= Ax + Bu, \quad y = Cx \\ A &= \begin{bmatrix} 0 & 1/C_r \\ -1/L_r & 0 \end{bmatrix}, \quad B = \begin{bmatrix} 0 \\ 1/L_r \end{bmatrix} \\ C &= [1 \ 0], \quad x = \begin{bmatrix} v \\ i \end{bmatrix}. \end{aligned} \quad (7)$$

Here, we assume that L_r and C_r are numerically equal. Then, $L_r = C_r = 1/\omega_1$. The state transition matrix $\Phi(t)$ is given by

$$\begin{aligned} \Phi(t) &= \mathcal{L}^{-1}[(sI - A)^{-1}] \\ &= \begin{bmatrix} \cos(\omega_1 t) & \sin(\omega_1 t) \\ -\sin(\omega_1 t) & \cos(\omega_1 t) \end{bmatrix}. \end{aligned} \quad (8)$$

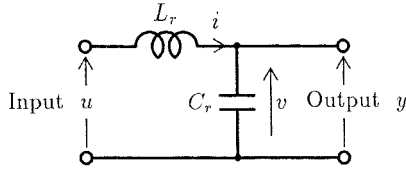


Fig. 5. Equivalent circuit of lossless resonant element.

In this expression, \mathbf{I} is the unit matrix. From (7) and (8), we can obtain the state equation in discrete-time domain as follows:

$$\begin{aligned} \mathbf{x}(n+1) &= \mathbf{P}\mathbf{x}(n) + \mathbf{Q}u(n) \\ y(n) &= \mathbf{C}\mathbf{x}(n) \end{aligned} \quad (9)$$

where

$$\begin{aligned} \mathbf{P} &= \Phi(T_c) = \begin{bmatrix} \cos(\omega_1 T_c) & \sin(\omega_1 T_c) \\ -\sin(\omega_1 T_c) & \cos(\omega_1 T_c) \end{bmatrix} \\ \mathbf{Q} &= \left[\int_0^{T_c} \Phi(\tau) d\tau \right] \mathbf{B} = \begin{bmatrix} 1 - \cos(\omega_1 T_c) \\ \sin(\omega_1 T_c) \end{bmatrix} \\ \mathbf{x}(n) &= \begin{bmatrix} v(n) \\ i(n) \end{bmatrix}. \end{aligned}$$

In these expressions, T_c is the calculation interval, $v(n)$, $i(n)$, and $u(n)$ are n th sampled values of v , i , and u , respectively. From expression (9), the state variables $\mathbf{x}(n+1)$ of $(n+1)$ th time step can be calculated consecutively using the state variables $\mathbf{x}(n)$ and input $u(n)$ of n th time step. This calculation is performed by using a DSP. The expressions for \mathbf{P} and \mathbf{Q} contain trigonometric functions, but these functions are constant for given values of the resonant frequency ω_1 and calculation interval T_c . Thus, the calculation of expression (9) requires just multiplication and addition. In this calculation procedure, the dc gain K_r of the lossless resonant element has been treated as unity. If $K_r \neq 1$, the calculated value of $y(n)$ obtained by (9) is multiplied by K_r .

As mentioned before, the resonant angular frequency ω_1 is set to the supply angular frequency ω_s . The calculation of expression (9) must be done every $\omega_s T_c$ rad of the phase angle of supply voltage. In the proposed control system, this calculation is started by an interrupt signal provided by the phase-locked loop (PLL) circuit, which is synchronized with the supply voltage. If the supply frequency becomes α times the nominal value, the calculation interval T_c becomes $1/\alpha$ times. In the calculation of (9), all the elements in matrices \mathbf{P} and \mathbf{Q} are treated as constant. Thus, the resonant frequency becomes α times its nominal value. In this way, the resonant frequency ω_1 always tracks the variation of the supply frequency ω_s automatically, ensuring the complete elimination of the control error in the ac input current.

B. Investigation of Stability

The characteristic polynomial appears in the denominator of expressions (2) and (5). Thus, the characteristic equation is given by

$$L_s s^3 + (R_s - K_p) s^2 + \omega_1^2 L_s s + \omega_1^2 (R_s - K_r - K_p) = 0. \quad (10)$$

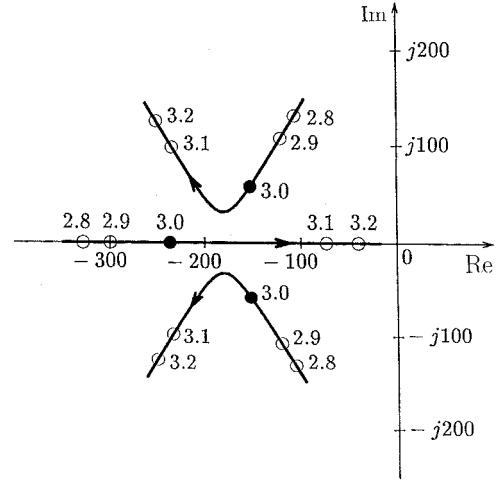
Fig. 6. Root locus for the variation of control gain K_r .

Fig. 6 shows the root locus of the ac input current control system shown in Fig. 4 for the variation of the control gain K_r in the range of $2.7 \leq K_r \leq 3.3$. The control gain K_p is set to -3 . The ac-side circuit parameters L_s and R_s are 6.28 mH and 0.4 Ω , respectively. The characteristic equation has a pair of complex roots and one real root. The pair of the complex roots moves from the right to left as the control gain K_r becomes large. In contrast to this, the real root moves from the left to right. When $K_r \simeq 3$, these three roots pass each other, and the distance of any one of the roots from the imaginary axis becomes large. This condition is the optimum from the view point of stability. Thus, K_r is set to 3 in the laboratory test systems.

In Fig. 6, the control gain K_p has been set to -3 . Under this condition, it is shown by the analysis using the root loci that the values of the real part of the roots when they pass each other on the complex plane becomes the largest with the negative sign. Thus, $K_r = 3$ and $K_p = -3$ is the optimum pair of the control gains to obtain the stable operation. This pair of the control parameters is used in the laboratory test systems and computer simulation.

V. EXPERIMENTAL INVESTIGATION

To confirm the effectiveness of the proposed control method, some experiments have been made employing a laboratory test system of the three-phase voltage-type PWM rectifier. The specifications of the laboratory test system are listed in Table I. The digital resonant element is implemented by a DSP (TI, TMS320C25). The calculation interval is 78.1 μ s when the supply frequency coincides with the nominal value 50 Hz.

Fig. 7 shows the steady-state waveform of the supply current i_s together with its reference i_s^* and the control error $(i_s^* - i_s)$. Here, i_s and i_s^* represent a phase component of \mathbf{i}_s and \mathbf{i}_s^* , respectively. We can see that the control error of the fundamental component is effectively eliminated by the proposed control method.

Fig. 8 shows a transient response of the supply current at a sudden change in the input current reference. In this experiment, the amplitude of i_s^* is suddenly increased at the

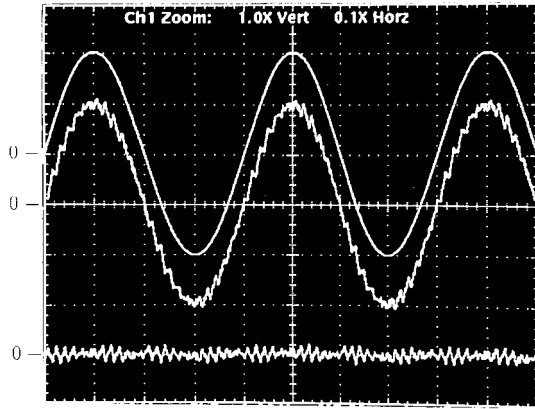


Fig. 7. Experimental waveform of input current in the steady state (three-phase rectifier, 10 A/div, 5 ms/div; upper: reference signal of input current i_s^* ; middle: detected input current i_s ; lower: control error $i_s^* - i_s$).

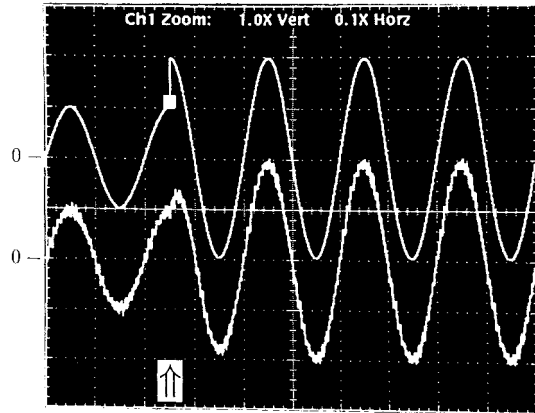


Fig. 8. Experimental waveform of input current at a sudden change in input current reference (three-phase rectifier, 10 A/div, 10 ms/div; upper: reference signal of input current i_s^* ; lower: detected input current i_s).

TABLE I
SPECIFICATIONS AND PARAMETERS OF LABORATORY
TEST SYSTEM OF THREE-PHASE RECTIFIER

AC Inductor	Inductance	$L_s = 6.28$ [mH]
	Resistance	$R_s = 0.4$ [Ω]
Supply Voltage and Frequency		100 [V], 50 [Hz]
Control Gains	Proportional Controller	$K_p = -3$ [V/A]
	Resonant Element	$K_r = 3$ [V/A]
DC Side Voltage		$V_d = 200$ [V]
Switching Frequency		1.2 [kHz]

instant denoted by an arrow. We can see that a stable operation is realized even under the transient condition. From these results, we can confirm the effectiveness of the proposed control method experimentally.

As mentioned in Section III-A, the proposed control method is directly applicable to single-phase voltage-type PWM rectifiers. A laboratory test system of the single-phase rectifier was constructed. The circuit parameters and control parameters are listed in Table II.

Fig. 9 shows an experimental result from this test system. In Fig. 9, a waveform of the input current i_s is shown with the waveforms of its reference signal i_s^* and the control error ($i_s^* - i_s$). Again, we can see the effectiveness of the proposed

TABLE II
SPECIFICATIONS AND PARAMETERS OF LABORATORY
TEST SYSTEM OF SINGLE-PHASE RECTIFIER

AC Inductor	Inductance	$L_s = 2.87$ [mH]
	Resistance	$R_s = 0.2$ [Ω]
Supply Voltage and Frequency		100 [V], 50 [Hz]
Control Gains	Proportional Controller	$K_p = -3$ [V/A]
	Resonant Element	$K_r = 3$ [V/A]
DC Side Voltage		$V_d = 200$ [V]
Switching Frequency		2.4 [kHz]

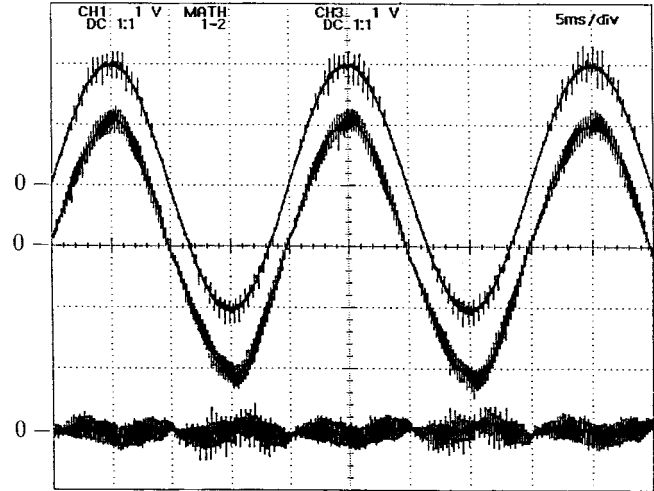


Fig. 9. Experimental waveform of input current in the steady state (single-phase rectifier, 10 A/div, 5 ms/div; upper: reference signal of input current i_s^* ; middle: detected input current i_s ; lower: control error $i_s^* - i_s$).

control method. However, as seen in Fig. 9, the supply current waveform contains a third harmonic component significantly. In the result shown in Fig. 9, the third harmonic component of the supply current is 4.0% of its fundamental component. This is because the voltage waveform of the single-phase power supply used in this experiment contains a third harmonic component. The effect of the harmonics of the supply voltage is investigated in Section VI.

VI. EFFECTS OF HARMONICS IN SUPPLY VOLTAGE

As seen in Fig. 9, the harmonic components in the supply voltage cause the waveform distortion of the input current. To confirm this, a result of computer simulation is shown in Fig. 10. The circuit parameters and control parameters listed in Table II are used in this simulation. The third harmonic component of the supply voltage is 3% of the fundamental components. In Fig. 10, we can see a waveform distortion in the input current waveform similar to the waveform distortion seen in Fig. 9. In this case, the third harmonic component is 5.62% of the fundamental component. From these results, we can conclude that the harmonic components in the supply voltage cause the waveform distortion of the input current.

To eliminate the waveform distortion due to the supply voltage harmonics, we introduce an additional lossless resonant element, the resonant frequency of which is set to the harmonic frequency as shown in Fig. 11. In this figure, a lossless resonant element of third harmonics is introduced in parallel with the proposed controller. As mentioned in

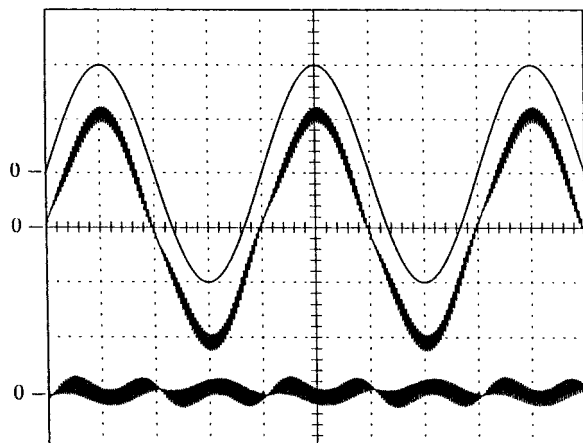


Fig. 10. Simulated waveform of input current in the steady state when supply voltage contains third harmonic component (single-phase rectifier, 10 A/div, 5 ms/div; upper: reference signal of input current i_s^* ; middle: detected input current i_s ; lower: control error $i_s^* - i_s$).

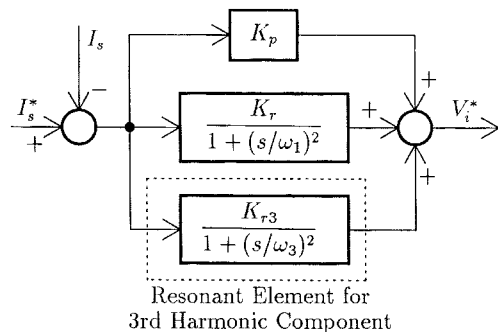


Fig. 11. Configuration of modified input current controller introducing additional resonant element for third harmonic component.

Section III, the resonant frequency component of the input current always coincides with its reference in the steady state. Although the reference signal of the third harmonic component is not shown explicitly, it is treated as zero in Fig. 11. Thus, the third harmonic component in the input current is eliminated completely. To confirm this, a result of the computer simulation employing the proposed control system in Fig. 11 is shown in Fig. 12. In this simulation, the control gain K_{r3} is 0.1. In this result, the third harmonic component is reduced to 0.74% of the fundamental component.

From these investigations, we can conclude that the additional lossless resonant element is effective in the elimination of the effects of the supply-voltage harmonics.

VII. CONCLUSION

In this paper, a new control strategy of the input current of the voltage-type PWM rectifiers employing the lossless resonant element has been proposed. Detailed implementation of the control method has been shown. The effectiveness of the control strategy has been confirmed by theoretical investigation and some results of the experimental work. In addition, the effects of the harmonic components in the supply voltage have been investigated. It has been shown that the harmonic components of the input current caused by the supply voltage harmonics can be eliminated by an additional resonant

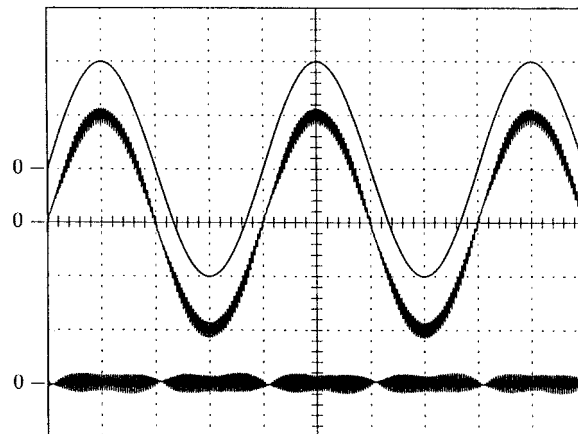


Fig. 12. Simulated waveform of input current in the steady state with modified input current controller (single-phase rectifier, 10 A/div, 5 ms/div; upper: reference signal of input current i_s^* ; middle: detected input current i_s ; lower: control error $i_s^* - i_s$).

element, the resonant frequency of which is set to the harmonic frequency.

The resonant element introduced in this paper has not been found in any current control circuits for power converters presented so far. From this point of view, this paper provides a new approach to digital current control.

REFERENCES

- [1] A. W. Green, J. T. Boys, and G. F. Gates, "Hysteresis current forced three phase voltage sourced reversible rectifier," *Proc. Inst. Elect. Eng.*, vol. 136, pt. B, no. 3, pp. 362–370, 1989.
- [2] J. W. Dixon and B. T. Ooi, "Indirect current control of a unity power factor sinusoidal boost type 3 phase rectifier," *IEEE Trans. Ind. Electron.*, vol. 35, pp. 508–515, Nov. 1988.
- [3] R. Wu, S. B. Dewan, and G. R. Slemon, "Analysis of an AC to DC voltage source converter using PWM with phase and amplitude control," *IEEE Trans. Ind. Applicat.*, vol. 27, pp. 355–364, Mar./Apr. 1991.
- [4] E. Wernekinck, A. Kawamura, and R. Hof, "A high frequency AC/DC converter with unity power factor and minimum harmonic distortion," *IEEE Trans. Power Electron.*, vol. 6, pp. 364–371, July 1991.
- [5] R. Wu, S. B. Dewan, and G. R. Slemon, "Analysis of a PWM AC to DC voltage source converter under the predicted current control with a fixed switching frequency," *IEEE Trans. Ind. Applicat.*, vol. 27, pp. 756–764, July/Aug. 1991.
- [6] T. Sukegawa, K. Kamiyama, J. Takahashi, T. Ikimi, and M. Matsutake, "A multiple PWM GTO line side converter for unity power factor and reduced harmonics," *IEEE Trans. Ind. Applicat.*, vol. 28, pp. 1302–1308, 1992.
- [7] A. Draou, Y. Sato, and T. Kataoka, "A new state feedback based transient control of PWM AC to DC voltage type converters," *IEEE Trans. Power Electron.*, vol. 10, pp. 716–724, Nov. 1995.



Yukihiko Sato (M'91) was born in Niigata, Japan, in 1963. He received the B.Eng., M.Eng., and D.Eng. degrees in electrical engineering from Tokyo Institute of Technology, Tokyo, Japan, in 1986, 1988 and 1995, respectively.

In 1988, he joined Tokyo Institute of Technology as a Research Associate. He is currently an Associate Professor in the Department of Electrical and Electronic Engineering. His primary research interests are the control and application of static power converters.

Dr. Sato is a member of the Institute of Electrical Engineers of Japan and the Japan Society of Power Electronics. He received the Prize Paper Award of the Industrial Power Converter Committee of the IEEE Industry Applications Society in 1995.



Tomotsugu Ishizuka was born in Tokyo, Japan, in 1970. He received the B.Eng. and M.Eng. degrees in electrical engineering from Tokyo Institute of Technology, Tokyo, Japan, in 1994 and 1996, respectively.

In 1996, he joined Toshiba Corporation Fuchu Works, Tokyo, Japan, where he has worked as an Electrical Engineer with the Power Electronics Development Group, Power Electronics Equipment Department.

Mr. Ishizuka is a member of the Institute of Electrical Engineers of Japan.



Kazuyoshi Nezu was born in Tokyo, Japan, in 1973. He received the B.Eng. and M.Eng. degrees in electrical engineering from Tokyo Institute of Technology, Tokyo, Japan, in 1996, and 1998, respectively.

He joined <AUTHOR: JOB TITLE?> Railway Technical Research Institute, Tokyo, Japan, in April 1998.

Mr. Nezu is a member of the Institute of Electrical Engineers of Japan.



Teruo Kataoka (M'78-SM'88-F'92) received the B.Eng, M.Eng, and D.Eng. degrees in electrical engineering from Tokyo Institute of Technology, Tokyo, Japan, in 1960, 1962, and 1965, respectively.

From 1965 to 1997, he was with the Tokyo Institute of Technology as a Research Associate, an Associate Professor, and then a Professor in the Department of Electrical and Electronic Engineering. In 1997, he retired from Tokyo Institute of Technology and joined Tokyo Denki University, Tokyo, Japan, where he is currently a Professor in

the Department of Electrical Engineering. He was the Editorial Director of the Institute of Electrical Engineers of Japan from 1988 to 1990. His research interests include electrical machines, static power conversion, variable-speed ac drive systems, and superconducting power apparatus.

Dr. Kataoka served as Chairman of the IEEE Industry Applications Society Tokyo Chapter, IEEE Tokyo Section, from 1992 to 1994. He has been a member of the Electrical Machines Committee of the IEEE Industry Applications Society since 1988. He received the 1982 IEEE Industry Applications Society Best Paper Award.